Author Accepted Manuscript. This article is published in Journal of Materials Science 56, 11698–11710 (2021),
https://doi.org/10.1007/s10853-021-06072-0

Interrelation among superstructural ordering, oxygen nonstoichiometry, and lattice strain of double perovskite $Sr_2FeMoO_{6-\delta}$ materials

Nikolay Kalanda[1,2*], Dmitry Karpinsky[1,3], Ivan Bobrikov[4], Marta Yarmolich[1], Victor Kuts[2], Lin Huang[5], Chanyong Hwang[6], and Dong-Hyun Kim[5]

[1] Scientific-Practical Materials Research Centre of NAS of Belarus, P.Brovka Str.19, 220072 Minsk, Belarus; E-mail: martochka_ymv@mail.ru
[2] National University of Science and Technology MISiS, Lenin Ave.4, 119049 Moscow, Russia; E-mail: viktor.kuts.3228@yandex.ru
[3] South Ural State University, Lenin Ave.76, 454080 Chelyabinsk, Russia; E-mail: dmitry.karpinsky@gmail.com
[4] Joint Institute for Nuclear Research, Joliot-Curie Str. 6, 141980 Dubna, Russia; E-mail: ivan.dubna@yandex.com
[5] Chungbuk National University, Chungdae-ro 1, Seowon-Gu,Cheongju, Chungbuk 28644, Korea; E-mail: donghyun@cbnu.ac.kr; l.huang0215@gmail.com
[6] Korea Research Institute of Standards and Science, 267 Ga-jeong-ro, Yuseong-gu, Daejeon 34113, Korea; E-mail: cyhwang@kriss.re.kr

*Contacting author:
E-mail: kalanda@physics.by
Tel: +375173670083; Fax: +375172151558

Abstract

Double perovskite ceramics $Sr_2FeMoO_{6-\delta}$ having different amount of antisite disordering and oxygen content are prepared by the solid-phase reaction method using $SrFeO_{2.52(3)}$ and $SrMoO_4$ initial reagents. X-ray and neutron diffraction techniques are used to estimate a modification in the structural parameters as a function of oxygen content and B–site cationic ordering. Reduction of oxygen content leads to an increase in the unit cell volume, which is mainly associated with an elongation of ***c*** –parameter of the tetragonal unit cell and relative expansion of the chemical bonds between Mo/Fe ions and apical oxygen ions. Superstructural ordering observed for the compounds causes a decrease in the unit cell volume, which is accompanied by a reduction in the length of the Mo/Fe – O bonds, located in the basal plane of oxygen octahedra. This modification of the unit cell parameters notably affects a character of the exchange interactions formed between B–site ions thus allowing to control magnetic and transport properties of $Sr_2FeMoO_{6-\delta}$ ceramics. It is found that comprehensive approach allows a consistent understanding of much debated structural/magnetic behaviors of double perovskite $Sr_2FeMoO_{6-\delta}$ systems, opening a venue for designing reliable devices based on the half-metallic double perovskite materials.

Keywords: double perovskite, strontium ferromolybdate, oxygen nonstoichiometry, Fe/Mo superstructural ordering, neutron diffraction, X–ray photoemission spectra

1. Introduction

Strontium ferromolybdate $Sr_2FeMoO_{6-\delta}$ (SFMO) with double perovskite structure is a prospective material for various applications in modern electronic industry, such as non-volatile magnetoresistive random-access memory (MRAM), magnetic read/write heads for hard disk drives, highly sensitive magnetic field sensors, electrodes for solid fuel cells, etc. [1–4]. These applications require the use of structurally perfect SFMO samples with Curie point above room temperature (T_C), high saturation magnetization (M_s), large degree of Fe/Mo cations superstructural ordering (P) as well as high spin polarization of free (delocalized) electrons [5–8]. The key task in the field of spintronics is to improve the technology for obtaining high-quality SFMO samples with reproducible magnetic and galvanomagnetic properties. The most crucial issue to get high degree of spin polarization in strontium ferromolybdate is the superstructural ordering of Fe/Mo cations located in the centers of oxygen octahedra with the required concentration of oxygen vacancies [7, 8].

Physico-chemical properties of the SFMO considerably depend on the oxygen stoichiometry, which influences the degree of superstructural ordering of iron and molybdenum cations, the orbital, charge and spin degrees of freedom, and therefore these properties particularly depend on the electronic exchange interaction between Fe^{3+} and Mo^{5+}. In a real crystal structure there is a number of various zero-dimensional defects, Mo_{Fe}, Fe_{Mo} antisite defects, as well as oxygen vacancies which cause a distortion of the crystal structure and lead to a redistribution of electron density and an appearance of cations of iron Fe^{2+} ($3d^6$ {S = 2}) and molybdenum Mo^{6+} ($4d^0$ {S = 0}). Since the diamagnetic molybdenum cation Mo^{6+} does not participate in exchange interactions, and only negative exchange interactions are possible between $Fe^{2+}(3d^6)$ or $Fe^{3+}(3d^5)$ ions, this leads to the formation of antiferromagnetic ordering. Therefore, any distortions of the crystal lattice caused by oxygen deficiency have a strong effect on the electrical transport and magnetic properties of strontium ferromolybdate [9, 10].

It is known that in the SFMO compound the density of electronic states N(E) near the Fermi level (E_F) is the key factor which determines the critical temperature (T_C) of the transition from paramagnetic to ferrimagnetic state, the saturation magnetization and galvanomagnetic properties. In turn, the value of E_F depends on the oxygen content (δ) and

the ordering of both oxygen vacancies and antisite defects Mo_{Fe}, Fe_{Mo} in the SFMO structure [6 – 8]. The possibility of simultaneous increase of the parameters δand P is in a contradiction with the results obtained by the authors of the work [11]; at the same time, the authors of other work [12] have declared similar results. We consider that this is due to the difference in the distribution of iron and molybdenum cations during their ordering associated with the concentration of oxygen vacancies.

Thus the functional dependence $\delta=f(Mo_{Fe}, Fe_{Mo})$ is determined by the oxygen nonstoichiometry, as well as the Fe/Mo superstructural ordering value. This circumstance leads to the fact that different synthesis conditions of strontium ferromolybdate, such as temperature, duration time and oxygen partial pressure $p(O_2)$ make it possible to obtain different values of the parameter P at a fixed value of oxygen vacancies and vice versa [13 – 15]. So, there is a number of works which declare various galvanomagnetic properties of the SFMO samples while the synthesis conditions are similar [15 –18]. One of the reasons why these materials are not widely used is the low reproducibility of the properties of materials obtained under similar conditions. Annealing temperature and time, type and flow of gas have a significant effect on the oxygen content of SFMO. This confirms the high sensitivity of the composite material to the synthesis conditions, on which the values of the parameters δ and P are largely depending [6–10].

The main purpose of this work is to determine a correlation between the oxygen non – stoichiometry and the degree of cationic ordering of iron and molybdenum ions in the SFMO compounds in order to obtain samples having optimal and reproducible magnetic and electro–physical properties.

Experimental

$Sr_2FeMoO_{6-\delta}$ polycrystalline samples were synthesized by solid-phase reaction technique [19, 20] using $SrFeO_{2.52(3)}$ and $SrMoO_4$ as precursors. The precursors were obtained by conventional ceramic technology from high purity simple oxides MoO_3, Fe_2O_3 and strontium carbonate $SrCO_3$. Starting reagents taken in stoichiometric amounts were thoroughly mixed using planetary mill in alcohol medium for 3 h. Resulting mixtures were dried at temperature of 350 K and pressed into pellets. Sintering of the $SrFeO_{3-x}$ and $SrMoO_4$ precursors was performed in air at 970 K and 1070 K for 20 h and 40 h respectively. To increase chemical homogeneity of the compounds, the mixtures were milled two times. The final synthesis of the compound $SrFeO_{3-x}$ was performed at T = 1470 K for 20 h in argon flow, for the compound $SrMoO_4$– at T = 1470 K for 40 h, with oxygen pressure $p(O_2)$ =

0.21×10^5 Pa followed by rapid tempering down to room temperature. The oxygen content in $SrFeO_{3-x}$ was determined by a weighing before and after its reduction to the SrO simple oxide and metallic Fe in the hydrogen atmosphere at 1373 K for 20 h. It was determined that strontium ferrite compound has a chemical composition $SrFeO_{2.52(3)}$.

During the synthesis procedure the strontium ferromolybdate was pressed into pellets with a diameter of 10mm and a thickness of 4–5 mm. $SrFeO_{2.52(3)}$ and $SrMoO_4$ taken in stoichiometric ratio were used as the starting reagents. The pellets were annealed in a gas mixture of 5%H_2/Ar at 1420 K for 5 h, followed by the tempering down to the room temperature. According to the XRD data, the initial samples of strontium ferromolybdate were single-phase compounds without the ordering of iron and molybdenum cations. The amount of oxygen content was estimated based on a complete reduction of the compound to the simple oxide SrO and the metals Fe and Mo in the hydrogen flow at 1373 K for 20 hours. The chemical formula $Sr_2FeMoO_{5.99(1)}$ attributed to the double perovskite has been determined. Density of the compound was $\rho = 87\%\rho_{theor}$, the average grain size was about 1μm, cations ordering P was about 56% (Fig. 1).

Ideally, the atoms of iron and molybdenum are arranged in the crystal lattice of $Sr_2FeMoO_{6-\delta}$ in the chess-like order − the superstructural ordering of iron and molybdenum cations. However, it often happens that the iron cation replaces the molybdenum cation, and vice versa, antisite defects arise (Fig. 2).

The phase purity and the unit cell parameters were determined based on the XRD data using the ICSD – PDF2 (Release 2000) database, FullProf [21] and PowderCell [22] software by the Rietveld technique on the basis of XRD data obtained in a Philips X'Pert MPD diffractometer using the Cu–Kα radiation at RT. XRD patterns were recorded at RT at a rate of 60 deg/h in the 10 – 90 deg angular range. The degree of the superstructural ordering of iron and molybdenum cations (P) was calculated using the formula $P=(2\cdot SOF - 1)\cdot 100\%$, where SOF is the occupation factor calculated based on the XRD data.

The powders were characterized by thermogravimetry (TGA) at a heating rate of 2.5 K/min in a flowing gas stream of 10%H_2/Ar using a SETARAM SetSys 16/18 system. The measurement error for a device with a mass variation range of ± 20 mg is 10 μg.

The neutron diffraction studies were performed in the temperature range of 5–500 K using a high resolution Fourier diffractometer (FDHR) installed in the IBR–2 pulsed reactor at the JINR (Dubna, Russia), for the investigations of crystal and magnetic structure of the $Sr_2FeMoO_{6-\delta}$ compounds. High-resolution neutron diffraction patterns were measured with

the detectors located at average neutron scattering angles of ± 152°, in the *d* –space range of0.6–4.5 Å. Neutron diffraction patterns were analyzed using FullProf software package.

X–ray photoemission spectra (XPS) measurements were carried out to investigate electronic structures of Fe and Mo edges by means of microfocused scanning X–ray source (PHI Quantera–II, Ulvac–PHI) over a sample area of 100 μm at room temperature with energy resolution of 0.48 eV.

Scanning electron microscopy (SEM) investigations have been carried out by means of the Vega 3 Tescan set up, which is a high-performance analytical thermionic emission SEM system, capable of operating in both high-vacuum and low-vacuum modes. It has a LaB6 filament with best resolution of 2 nm at 30 kV in high-vacuum mode and 2.5 nm at 30 kV in low-vacuum mode.

The Curie temperature was determined through the analysis of the temperature dependences of the magnetization of the $Sr_2FeMoO_{6-\delta}$ samples by the ponderomotive technique in the temperature range from 77–800 K in an applied magnetic field of 0.86 T, using the PPMS universal setup by the Cryogenic Ltd.

Results and Discussion

Analysis of the saturation rates of the oxygen index and the degree of cations ordering of $Sr_2FeMoO_{5.99(1)}$ samples was performed based on the isothermal dependencies having the form: $(6-\delta) = f_1(t)$ and $P = f_2(t)$. The behavior of the $(6-\delta) = f_1(t)$ dependencies has been studied under conditions of isothermal annealing of the samples $Sr_2FeMoO_{5.99(1)}$ at different temperatures in a flow of the 5%H_2/Ar gaseous mixture. Temperature is increased at a rate of 12 K/min. The change in the oxygen index reaches the saturation value of 5.96(2) at T = 1370 K after annealing for 18.2 hours, while at an increased annealing temperature of T = 1470 K for 13.6 hours the oxygen index becomes 5.92(3) (see Fig. 3). The dependence $(6-\delta) = f_1(t)$ was fitted with a function $6-\delta = (6-\delta_o)\exp(-t/\tau_o)$, where τ_o – relaxation time of oxygen desorption, $(6-\delta_o) = 5.99(1)$ – oxygen content at the beginning of the measurements (Table 1).

Kinetics of the Fe/Mo cations ordering in the $Sr_2FeMoO_{5.99(1)}$ compounds has been studied analyzing the function $P = f_2(t)$, constructed for the compounds annealed in gaseous mixture of 5%H_2/Ar at different temperatures during 120 h with a step of 15 h. After annealing the compounds were tempered down to room temperature in the same atmosphere. According to the XRD data, the superstructural ordering degree of Fe/Mo cations has non-linear character whereas reaching the maximum values of P parameter requires a long time annealing (Fig. 4). It was observed that the value of P parameter is growing with an increase

in a temperature of isothermal annealing and reaches the magnitudes of P_{max} = 88% at T = 1320 K for t = 120 h, P_{max}= 92% at T = 1420 K for t = 100 h, while the value P_{max}= 90% at T = 1470 K for t = 45 h. It is considered that the value of P_{max} at T = 1470 K which is lower than the value at T = 1420 K is caused by the effect of thermal energy which destroys the chain ordering of Fe and Mo cations, placed in the staggered arrangement. At the approximation of $dP/dt=f_2(t)$ by the function $dP/dt= \exp(-t/\tau_p)\, dP_o/dt$, where τ_p is the relaxation time of the Fe/Mo cations superstructural ordering, and dP_o/dt is the derivative of the superstructural cations ordering at the starting time the value of the parameter τ_p has been calculated at various annealing temperatures (see Table 1).

Comparison of the kinetics of changes in oxygen nonstoichiometry and the degree of superstructural ordering of Fe/Mo cations indicates that the rate of oxygen desorption is several times higher than the rate of superstructural ordering of cations (Fig. 5). It should be pointed out that the rate of increase in the Curie temperature (T_C) correlates with the rate of growth of P. Nevertheless, it is clearly seen from Fig. 5 that the impetus for an increase in the values of P and T_C was a decrease in the oxygen concentration in the anionic sublattice of the magnetic.

To further understand the effect of oxygen non – stoichiometry and cation ordering on the crystal structure, we have carried out heat treatment for the sample, allowing an oxygen desorption to vary the oxygen index. The obtaining of strontium ferromolybdate with different δ and P values was carried out by annealing at 1420K in a flow of a gas mixture of 5% H_2/Ar for 15 hours – SFMO –1 ($Sr_2FeMoO_{5.97(5)}$ with P = 60%), 18 hours – SFMO – 2($Sr_2FeMoO_{5.94(4)}$ with P = 67%), 21 hours – SFMO – 3 ($Sr_2FeMoO_{5.94(1)}$ with P = 78%), 50 hours – SFMO – 4 ($Sr_2FeMoO_{5,94(1)}$ with *P* = 86%), 90 hours– SFMO – 5 ($Sr_2FeMoO_{5.94(1)}$ with P = 93%). As expected based on the previous observation in the cases of annealing, it has been found that P increases from 60% to 93% and 6–δ decreases from 5.97(5) to 5.94(1) with respect to the heat treatment time due to the increasing oxygen desorption. The presence of XRD peak at (101) indicates the formation of the Fe/Mo cations superstructural ordering (Fig. 6).

The crystal structure of the SFMO compound is similar to the structure of the ideal ABO_3 perovskite. While in contrast to ABO_3, the unit cell of strontium ferromolybdate at room temperature is characterized by the metric $\sqrt{2a_p}\cdot\sqrt{2a_p}\cdot 2a_p$, where a_p is the parameter of the primitive perovskite unit cell [23]. Phase purity of the compounds SFMO –1, 2, 3, 4, 5 was confirmed based on the neutron diffraction data, where unit cell parameters, ion occupation values, and the bond lengths were calculated. It was established that at

temperatures less than $T < T_C$ the compounds have tetragonal symmetry of the unit cell (described by the space group I4/m), and at temperatures $T > T_C$ (e.g. T = 500 K) the samples are characterized by cubic symmetry (space group *Fm –3m*, Fig. 7). The calculated parameters of the unit cell cells are presented in the Table 2.

Two main space groups *I4/m* and *I4/mmm* with the same metrics ($\sqrt{2a_p}\cdot\sqrt{2a_p}$ $2a_p$) have been considered, in order to describe tetragonal distortions of the SFMO compounds. The main difference between the mentioned space groups is associated with the coordinates of oxygen ions located in different structural positions O1 and O2, Table 2 [24, 25]. This difference is associated with two types of asymmetrically distorted oxygen octahedra FeO_6 and MoO_6which are located in chess-like order and have apical oxygen ions O1 aligned along ***c*** –axis, while four oxygen ions O2 are located in basal ***ab*** plane of oxygen octahedra. In the *I4/m* space group the above indicated position is characterized by the set of coordinates (*x, y, 0*), while in the space group *I4/mmm* the dependent set of coordinates associated with the same oxygen ion is (*x, x, 0*) which means similar values for *x* and *y* coordinates. Two independent coordinates of the oxygen ions allowed in the space group *I4/m* result in a possibility of a rotation of oxygen octahedral in the ***ab*** plane, while such structural distortion is forbidden in the *I4/mmm* space group.

The diffraction patterns obtained for the compounds SFMO–1, 2, 3, 4, 5 were analyzed using the both mentioned space groups. The amount of antisite defects taken from the XRD data as well as the value of oxygen deficiency taken from the TGA data were fixed during refinement procedure. The reliability factors calculated using the space group *I4/m* were predictably lower as compared to those obtained for the model with the space group *I4/mmm*. Additionaly, the profile of the neutron diffraction pattern, taking into account the neutron reflections 121|013, 213|301 associated with the rotation of the oxygen octahedron around the c axis, could be well described only within the space group *I4 / m* (Fig. 8). The diffraction patterns were successfully refined using the same space group *I4/m*, which confirms structural stability of the tetragonal phase in the temperature range 5 – 300 K.

Based on the fact that the binding energies of the oxygen ions O1 and O2 are practically equal, the oxygen vacancies in the unit cell of SFMO can form both in the base plane (chemical bonds Fe/Mo – O2) as well as along the OZ axis in (Fe/Mo – O1) [26 – 28]. While based on the analysis of the neutron diffraction data one can conclude about dominant location of oxygen vacancies in the structural positions O2, and this conclusion is valid for all the studied compounds, SFMO –1, 2, 3, 4, and SFMO –5.

The values of the reliability factors presented in the Table 2 (R_{wp}< 6% and $\chi^2 < 4$) exhibit a well match between the experimental and calculated data, which allows us to calculate the parameters of the unit cell lattice, coordinates, and the bond lengths with high accuracy.

The formation of oxygen vacancies leads to an increase in the unit cell parameters, which, in turn, contributes to an increase in the bond lengths Fe–O1, Fe–O2, Mo–O1, and Mo–O2, thereby increasing the unit cell volume (Table 2). It should be noted that the lattice parameter ***a*** increases faster than parameter ***c*** as concentration of defects δ increases (Fig. 9, Table 2).

It was found that an increase in the Fe/Mo cation ordering leads to nonuniform decrease in the and ***c*** unit cell parameters, viz. the bond length Fe – O1 decreases and Mo – O1 increases, which indicates compression of FeO_6 octahedra and elongation of the MoO_6 octahedra along the OZ axis. Thus, apical anions O1 of the FeO_6 oxygen octahedra located along the tetragonal axis ***c*** become more separated from the iron cations, while four O2 anions located in the ***ab*** plane of the octahedra become to be closer to the iron cation. In the MoO_6 octahedron the situation is reversed; the anions O1 are located at a larger distance from the Mo cation than four O2 anions located in the ***ab*** plane.

Despite the presence of oxygen vacancies, the unit cell volume decreases with an increase in the P value, implying an increase of chemical bond covalency associated with an overlapping of the electronic orbitals of cations and anions. The Fe/Mo cation ordering strongly affects the unit cell parameters, compared to the influence of oxygen vacancies. It should be noted that compounds with high P values are characterized by distinct differences in the bond lengths of Fe – O and Mo – O, which is found to be valid for both positions of oxygen ions (Fig.10).

It can be assumed that the noticeable difference in the mentioned bond lengths is associated with the redistribution of the electron charge density towards to Mo ions, due to their higher electronegativity as compared to iron ions. As the result, the chemical bond Mo–O1 is more covalent than the Fe – O1 one. Thus, an increase in the value of P leads to a redistribution of the electron density and the transition of a part of the molybdenum cations to the higher-spin state $Mo^{6+} \rightarrow Mo^{5+}$, which in turn increases the degree of population of t_{2g} orbitals of molybdenum cations [28 – 30]. This fact is confirmed by the results of the XPS measurements.

Fig. 11 shows the XPS spectra of core levels of Fe2p (a) and Mo3d (b) for the SFMO–1, 3, and 5 samples. The results of XPS measurements performed for the compounds SFMO–1,

3, and SFMO – 5 has allowed to clarify electronic state of the molybdenum and iron cations. It was found that the core level of Fe_{2p} is a spin-orbit doublet and it consists of two $Fe_{2p3/2}$ and $Fe_{2p1/2}$ sublevels (Fig. 11 a). When processing the energy spectra of iron, the distance between the doublets was set equal to 13.6 eV and the ratio of the peaks $Fe_{2p3/2}$/ $Fe_{2p1/2}$ was 2/1 [31]. Analysis of the XPS spectra of the SFMO–1, 3, and 5 compounds, has allowed to determine that the Fe_{2p} spectrum is a superposition of four components– two for $Fe_{2p3/2}$ and two for $Fe_{2p1/2}$, indicating the valence states of Fe^{3+} and Fe^{2+} (respective areas are highlighted in red and blue colors, Fig. 11 a) [32–35]. Thus, it was determined that the concentration of Fe^{2+}ions increases with decreasing of the parameter P (Table 3).

Similar situation is observed for the core level of Mo_{3d}, which is a spin-orbit doublet and consists of two $Mo_{3d5/2}$ and $Mo_{3d3/2}$ sublevels (Fig. 11b). The XPS data have been analyzed given the distance between the doublets is equal to 3.13 eV and the ratio of the peaks $Mo_{3d5/2}$/$Mo_{3d3/2}$ is 3/2 [31]. The XPS spectra of the Mo_{3d} ion in the compounds SFMO–1, 3, 5 has been refined assuming a superposition of four components: two for $Mo_{3d3/2}$ and two for $Mo_{3d5/2}$, indicating Mo^{5+} and Mo^{6+} valence states (respective regions are marked by red and blue lines, Fig. 11b) [32–35]. The spectral features denoting an increase in the amount of Mo^{6+} ions with a decrease in the value of P have been observed (Table 3). The XPS data have confirmed the absence of iron and molybdenum ions having Fe^0 and Mo^{4+} electronic configurations, which confirms the single-phase nature of the obtained compound SFMO–1, 3, 5, which is in good agreement with the results of the XRD data.

Thus, in the compounds having low values of P and δ, the iron and molybdenum cations have the mixed valence states with a larger fraction of $Fe^{2+}(3d^6)$ and $Mo^{6+}(4d^0)$ cations. In this case, the magnetic moment of the molybdenum cation (Mo^{6+}) is equal to zero, and the $\mu(Fe^{2+})$ is equals 4 μ_B. Therefore, the total magnetic moment of strontium ferromolybdate is 4 μ_B/f.u. Increase in the values of P and δ leads to redistribution of the charge density with the predominant formation of iron $Fe^{3+}(3d^5)$ and molybdenum cations and Mo^{5+} $(4d^1)$.

The magnetic structure of the compounds SFMO–1, 2, 3, 4, and 5 was determined based on the neutron diffraction data using FullProf software package. It was found that the most intensive reflections observed at 5 K and 300 K correspond to magnetic ordering at distance 1.8, 2.38, and 4.55 Å. At temperatures above T_C (viz. T=500 K), the mentioned reflections were not detected, the additional reflections ascribed to superstructure magnetic order was not detected, which points at ferrimagnetic structure with a wave vector k = [0,0,0] (Fig. 8).

Using the determined propagation vector, we have performed the symmetry analysis of the possible magnetic ordering schemes which has been carried out by means of the SARAh

program [36]. The theory and details about this method application can be found, for example, in [37]. For both magnetic ***2a*** and ***2b*** sites, the ordering occurs with the same irreducible representations (IRs). There are three IRs, for which the decomposition for both sites has non-zero coefficients. From the analysis it follows that, the magnetic transition should involve one or more of the following three IRs: ***Γ1***, ***Γ3***, and ***Γ7*** (in notation of SARAh). The IR of ***Γ1*** implies the orientation of the magnetic moments of atoms only along the *c* – axis, ***Γ3*** – along *a*–axis and ***Γ7***– along *b* –axis. The best fit was achieved assuming both IRs ***Γ1*** and ***Γ7***, in this case the magnetic moments are located in the plane (*bc*) and are parallel to the directions [011] (Fig. 12).

When calculating the magnetic moment of the iron and molybdenum sublattice at T=300 K, it was found that the values of the magnetic moment are monotonically decreasing from 2.1 μ_B/f.u. to1.6 μ_B/f.u. for Fe and from 0.3 μ_B/f.u. to 0.1 μ_B/f.u. for Mo with an increase in the oxygen nonstoichiometry coefficient from $\delta = 0.025$ to $\delta = 0.06$. When the P value increases and at a constant $\delta = 0.06$, the reverse trend is observed, in which the values of the magnetic moment are monotonically increasing from 1.6 μ_B/f.u. to 2.5 μ_B/f.u. for Fe and from 0.1 μ_B/f.u. to 0.4 μ_B/f.u. for Mo (Table 2).

It should be noted that the magnitude of the error in the magnetic moment of molybdenum (~10%) is quite large due to multiple correlations with other refined parameters. Therefore, strictly speaking, it is difficult to establish exact values of the magnetic moment of molybdenum. A similar situation is observed at helium temperature (5K).

Conclusions

The effects of oxygen non–stoichiometry and Fe/Mo cation ordering on crystalline and magnetic structure of the SFMO double perovskites have been comprehensively studied by combining XRD, neutron diffraction, and XPS. Study of the changes occurred in oxygen nonstoichiometry and the degree of cations ordering has allowed to determine that the oxygen desorption rate is several times larger than the superstructural ordering rate of iron and molybdenum ions.

In the compounds with low values of P and δ, the iron and molybdenum cations have a mixed valence states with a large fraction of Fe^{2+} ($3d^6$) and Mo^{6+} ($4d^0$) cations. Increase in the values of P and δ leads to a redistribution of the charge density with the predominant formation of iron Fe^{3+}($3d^5$) and molybdenum Mo^{5+}($4d^1$) cations. Analysis of magnetic structure performed using irreducible representation methods has allowed to find out that the best agreement was achieved when the magnetic moments are located in the (***bc***) planes and

parallel to the direction [011]. It was found that the magnetic moment of Fe cations monotonically decreases while for Mo ions the magnetic moments increases with increasing of δ, while the opposite tendency is observed for the P parameter.

Our systematic approach allows a comprehensive and consistent analysis of the structural and magnetic properties of the SFMO compound, shedding a light in application of double perovskite materials for future spintronic applications.

Acknowledgments

The work was supported by the European project H2020–MSCA–RISE–2017–778308–SPINMULTIFILM, and it has been realized with a financial support of the Ministry of Science and Higher Education of the Russian Federation as a part of the State Assignment (basic research, Project No. 0718-2020-0031 "New magnetoelectric composite materials based on oxide ferroelectrics having an ordered domain structure: production and properties"). This work was also supported by Korea Research Foundation (NRF) grants No. 2018R1A2B3009569, No. 2020R1A4A1019566 and a KBSI Grant D010200.

Compliance with ethical standards

Conflict of Interest: The authors declare that they have no conflict of interest.

References

[1] dos Santos-Gómez L, León-Reina L, Porras-Vázquez JM et al (2013) Chemical stability and compatability of double perovskite anode materials for SOFCs. Solid State Ionics, 239:1 –7. https://doi.org/10.1016/j.ssi.2013.03.005

[2] Kovalev LV, Yarmolich MV, Petrova ML et al (2014) Double perovskite Sr_2FeMoO_6 films prepared by electrophoretic deposition. ACS Appl. Mater. Interfaces. 6:19201–19206. https://dx.doi.org/10.1021/am5052125

[3] Kalanda N, Yarmolich M, Teichert S et al (2018) Charge transfer mechanisms in strontium ferromolybdate with tunneling barriers. J. Mater. Sci. 53:8347–8354. https://doi.org/10.1007/s10853-018-2148-0

[4] Kalanda NA, Kovalev LV, Waerenborgh JC et al (2015) Interplay of superstructural ordering and magnetic properties of the $Sr_2FeMoO_{6-\delta}$. Sci. Adv. Mater. 7:446 –454. https://doi.org/10.1166/sam.2015.2134

[5] Serrate D, De Teresa JM, Ibarra MR (2007) Double perovskites with ferromagnetism above room temperature. J. Phys.: Condens. Matter. 19:023201. https://doi.org/10.1088/0953 –8984/19/2/023201

[6] Topwal D, Sarma DD, Kato H et al (2006) Structural and magnetic properties of $Sr_2Fe_{1+x}Mo_{1-x}O_6$ [−1<x<0.25]. Phys. Rev. B73:094419. https://doi.org/10.1103/physrevb.73.094419

[7] Chan TS, Liu RS, Hu SF, et al (2005) Structural and physical properties of double perovskite compounds Sr_2FeMoO_6 (M = Mo, W). Mater. Chem. Phys. 93:314 – 319. https://doi.org/10.1016/j.matchemphys.2005.03.060

[8] Rager J, Zipperle M, Sharma A et al (2004) Oxygen stoichiometry in Sr_2FeMoO_6, the determination of Fe and Mo valence states, and the chemical phase diagram of SrO – Fe_3O_4 – MoO_3. J. Am. Ceram. Soc. 87:1330 – 1335. https://doi.org/10.1111/j.1151 – 2916.2004.tb07730.x

[9] Allub R, Navarro O, Avignon M et al (2002) Effect of disorder on the electronic structure of the double perovskite Sr_2FeMoO_6. Physica B: Condens. Matter.320:13–17. https://doi.org/10.1016/S0921 –4526(02)00608 –7

[10] Liscio F, Bardelli F, Meneghini C et al (2006) Local structure and magneto-transport in Sr_2FeMoO_6 oxides. Nucl. Instrum. Methods Phys. Res. B. 246:189 – 193. https://doi.org/10.1016/j.nimb.2005.12.033

[11] Stoeffler D, Colis S (2005) Oxygen vacancies or/and antisite imperfections in Sr_2FeMoO_6 double perovskites: an *ab initio* investigation. J. Phys.: Condens. Matter. 17:6415. https://doi.org/10.1088/0953 –8984/17/41/012

[12] Klencsár Z, Németh Z, Vértes A et al (2004) The effect of cation disorder on the structure of Sr_2FeMoO_6 double perovskite. J. Magn. Magn. Mater. 281:115 – 123. https://doi.org/10.1016/j.jmmm.2004.04.097

[13] Kalanda N, Suchaneck G, Saad A et al (2010) Influence of oxygen stoichiometry and cation ordering on magnetoresistive properties of$Sr_2FeMoO_{6\pm\delta}$. Mater. Sci. Forum. 636 –637:338 –343. https://doi.org/10.4028/www.scientific.net/MSF.636 –637.338

[14] Hemery EK, Williams GVM, Trodahl HJ (2006) The effect of the preparation method and grain morphology on the physical properties of A_2FeMoO_6 (A = Sr, Ba). Curr. Appl. Phys. 6:312 –315. https://doi.org/10.1016/j.cap.2005.11.007

[15] Matsuda Y, Karppinen M, Yamazaki Y et al (2009) Oxygen-vacancy concentration in $A_2MgMoO_{6-\delta}$ double-perovskite oxides. J. Solid State Chem. 182:1713–1716. https://doi.org/10.1016/j.jssc.2009.04.016

[16] Sharma A, Mac Manus-Driscoll JL, Branford W (2005) Phase stability and optimum oxygenation conditions for Sr_2FeMoO_6 formation.Appl. Phys. Lett.87:112505. https://doi.org/10.1063/1.2048810

[17] Kircheisen R, Töpfer J (2012) Nonstoichiometry, point defects and magnetic properties in $Sr_2FeMoO_{6-\delta}$ double perovskites. J. Solid State Chem. 185:76–81. https://doi.org/10.1016/j.jssc.2011.10.043

[18] Niebieskikwiat D, Caneiro A, Sánchez RD et al (2001) Oxygen-induced grain boundary effects on magnetotransport properties of $Sr_2FeMoO_{6+\delta}$. Phys. Rev. B., 64: 180406. https://doi.org/10.1103/PhysRevB.64.180406

[19] Kalanda N, Demyanov S, Masselink W, et al (2011) Interplay between phase formation mechanisms and magnetism in the Sr_2FeMoO_6 metal–oxide compound. Cryst. Res. Technol. 2011:463–469. https://doi.org/10.1002/crat.20100213

[20] Jurca B, Berthon J, Dragoe N et al (2009) Influence of successive sintering treatments on high ordered Sr_2FeMoO_6 double perovskite properties. J. Alloys Compd. 474:416 –423. https://doi.org/10.1016/j.jallcom.2008.06.100

[21] Rodríguez-Carvajal J (2001) Recent developments of the program FULLPROF. Newsletter in Commission on Powder Diffraction (IUCr). 26

[22] Kraus W, Nolze G. (1996) POWDER CELL – a program for the representation and manipulation of crystal structures and calculation of the resulting X –ray powder patterns. J. Appl. Crystallogr. 29:301 – 303. https://doi.org/10.1107/S0021889895014920

[23] Nakayama S, Nakagawa T et al (1968) Neutron Diffraction Study of $Sr_2(FeMo)O_6$. J. Phys. Soc. Jpn. 24:219 –220. https://doi.org/10.1143/JSPS.24.219

[24] Sánchez D, Alonso JA, García-Hernández M et al (2002) Origin of neutron magnetic scattering in antisite-disordered Sr_2FeMoO_6 double perovskites. Phys. Rev. B. 65:104426. https://doi.org/10.1103/PhysRevB.65.104426

[25] Chmaissem O, Kruk R, Dabrowski B et al (2000) Structural phase transition and the electronic and magnetic properties of Sr_2FeMoO_6. Physical Review B.62:14197. https://doi.org/10.1103/PhysRevB.62.14197

[26] Feng XM, Liu GY, Huang QZ et al (2006) Influence of annealing treatment on structural and magnetic properties of double perovskite Sr_2FeMoO_6. Transactions of Nonferrous Metals Society of China. 16:122 –126. https://doi.org/10.1016/S1003 – 6326(06) 60021 –6

[27] Chung MK, Huang PJ, Li WH et al (2006) Crystalline and magnetic structures of Sr_2FeMoO_6 double perovskites. Physica B: Condensed Matter. 385:418 – 420. https://doi.org/10.1016/j.physb.2006.05.140

[28] Kalanda N, Turchenko V, Karpinsky D et al (2019) The role of the Fe/Mo cations ordering degree and oxygen non–stoichiometry on the formation of the crystalline and magnetic structure of $Sr_2FeMoO_{6–\delta}$. Phys. Status Solidi B. 256:1800278.https://doi.org/10.1002/pssb.201800278

[29] Menendez N, Garcia –Hernandez M, Sanchez D et al (2004) Charge transfer and disorder in double perovskites. Chem. Mater.16:3565 –3572. https://doi.org/10.1021/cm049305t

[30] Lindén J, Yamamoto T, Karppinen, M et al (2000) Evidence for valence fluctuation of Fe in $Sr_2FeMoO_{6–w}$ double perovskite. Appl. Phys. Lett. 76:2925. https://doi.org/10.1063/1.126518

[31] Goldstein J, Newbury DE, Joy DC, Lyman CE, Echlin P, Lifshin E, Sawyer L, Michael JR (2003) Scanning Electron Microscopy and X–ray Microanalysis, Kluwer Academic / Plenum Publishers, New York

[32] Yarmolich M, Kalanda N, Demyanov S et al (2016) Charge ordering and magnetic properties in nanosized $Sr_2FeMoO_{6–\delta}$ powders. Phys. Status Solidi B., 253:2160 – 2166.https://doi.org/10.1002/pssb.201600527

[33] Raekers M, Kuepper K, Hesse H et al (2006) Investigation of chemical and grain boundary effects in highly ordered Sr_2FeMoO_6: XPS and Mossbauer studies. J. Optoelectron. Adv. Mater. 8:455 –460. ISSN: 1454 –4164

[34] Kalanda N, Yarmolich M, Kim D-H et al (2020) Valence state of iron and molybdenum cations under conditions of anionic deficiency in $Sr_2FeMoO_{6–\delta}$. Phys. Status Solidi B. 257:1900387. https://doi.org/10.1002/pssb.201900387

[35] Kang J–S, Kim JH, Sekiyama A et al (2002) Bulk-sensitive photoemission spectroscopy of A_2FeMoO_6 double perovskites (A = Sr, Ba). Phys. Rev. B. 66:113105. https://doi.org/10.1103/PhysRevB.66.113105

[36] Wills AS (2000) A new protocol for the determination of magnetic structures using simulated annealing and representational analysis (SARAh). Physica B: Condensed Matter. 276:680 –681. https://doi.org/10.1016/S0921 –4526(99)01722 –6

[37] Bertaut EF (1971) Magnetic structure analysis and group theory J. Phys. Colloques 32:C1–462– C1–470. https://doi.org/10.1051/jphyscol:19711156

Figure Captions

Figure 1 SEM image obtained for compound $Sr_2FeMoO_{5.99(1)}$.

Figure 2 Schematic representation of the deficiency and the formation of superstructural ordering of iron and molybdenum cations in the crystal structure of strontium ferromolybdate during its synthesis: a) the powder is enriched in iron, $Sr_2Fe_{1+x}Mo_{1-x}O_{6-\delta}$; b) $Sr_2FeMoO_{6-\delta}$, P <100%; c) $Sr_2FeMoO_{6-\delta}$, P = 100% (the square represents the vacancy for molybdenum, strontium is in the center of each cell, but not shown for clarity).

Figure 3 The dependencies of oxygen content as a function of annealing time of $Sr_2FeMoO_{5.99(1)}$ compounds in a stream of a mixture of inert gases 5%H_2/Ar with a heating rate of 12 K/min followed by isothermal annealing at different temperatures.

Figure 4 Time dependencies of the superstructural ordering degree of the Fe/Mo cations obtained during the thermal treatment of $Sr_2FeMoO_{5.99(1)}$ compounds in a stream of the 5%H_2/Ar gaseous mixture with a heating rate of 12 K/min. The inset shows the first derivative of the time dependencies of the Fe/Mo cations superstructural ordering degree.

Figure 5 Fe/Mo cations ordering degree, the temperature Curie and oxygen index 6–δ with respect to the heat treatment time.

Figure 6 XRD pattern of the $Sr_2FeMoO_{5.94(1)}$ compound obtained at room temperature. The inset shows the X–ray reflection (101), which relates to samples with different degrees of superstructural ordering of Fe/Mo cations.

Figure 7 a) tetragonal lattice (space group *I4/m*); b) cubic lattice (space group $Fm\bar{3}m$).

Figure 8 a) Neutron diffraction patterns obtained for the SFMO –1,b) SFMO –3, and c) SFMO – 5 compounds at temperature of 5 K. Bragg positions attributed to the structural tetragonal phase are marked by vertical ticks; ticks at bottom row are associated with the magnetic structure. The inset shows the selected peaks associated with oxygen octahedra rotation (*) and cationic and magnetic order (•) at temperatures 5 K, 300 K and 500 K.

Figure 9 The unit cell parameters (a, c, V) calculated at T=300 K for the compounds SFMO–1, 2, 3, 4 и 5 with different values of δ depending on the values of the Fe/Mo cations ordering.

Figure 10 Dependencies of the Fe – O1, Fe – O2, Mo – O1 and Mo – O2 bond lengths obtained at T=300 K depending on the Fe/Mo cations superstructural ordering.

Figure 11 XPS spectra of the core levels of a) Fe_{2p}, and b) Mo_{3d} of the SFMO– 1, 3 and 5 compounds.

Figure 12 Tetragonal lattice (space group *I4/m*) with magnetic moments ascribed to the Fe and Mo ions and aligned along the direction [011].

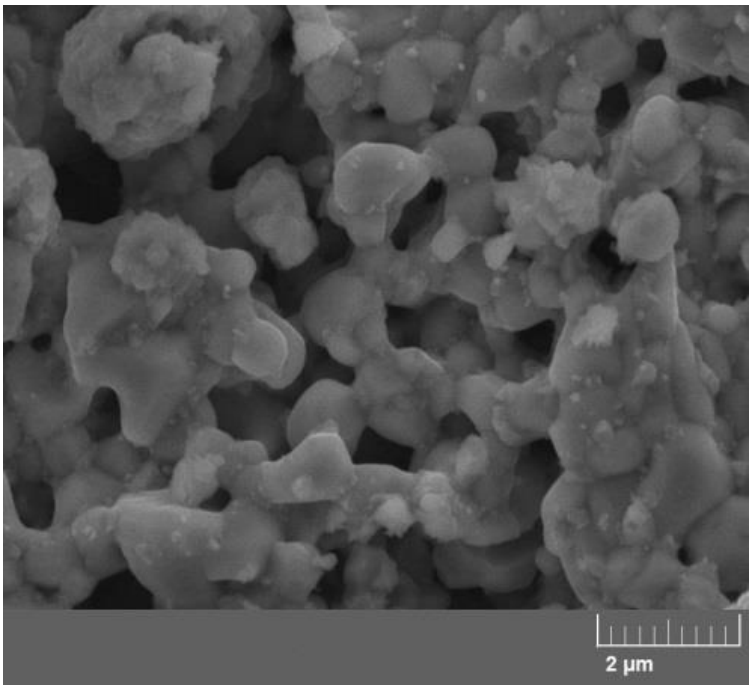

Figure 1

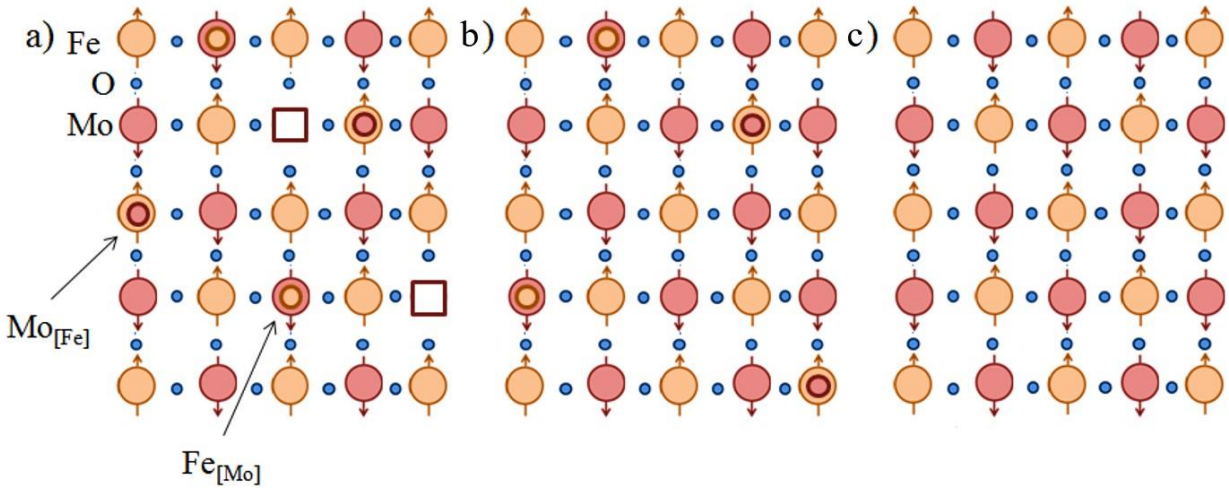

Figure 2

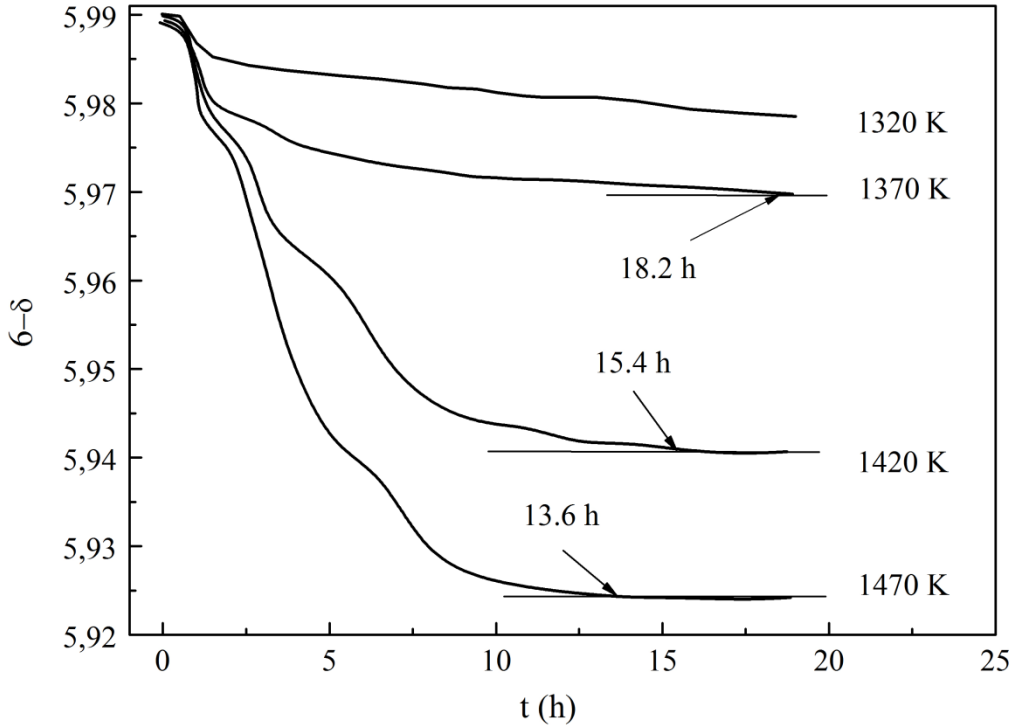

Figure 3

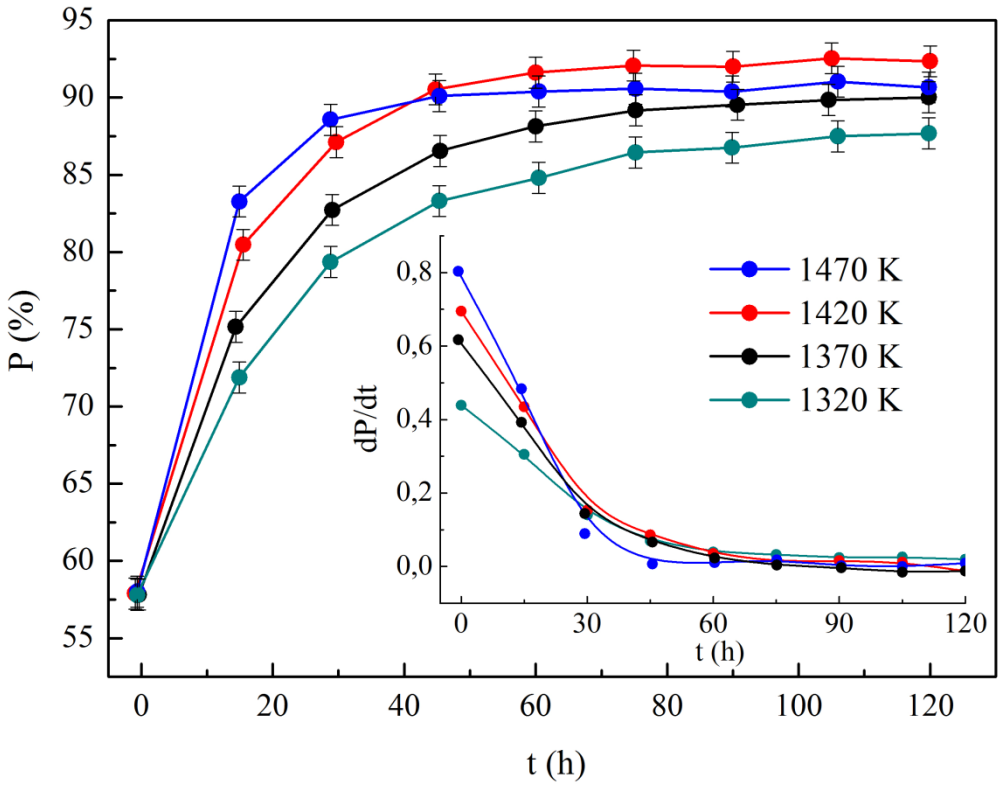

Figure 4

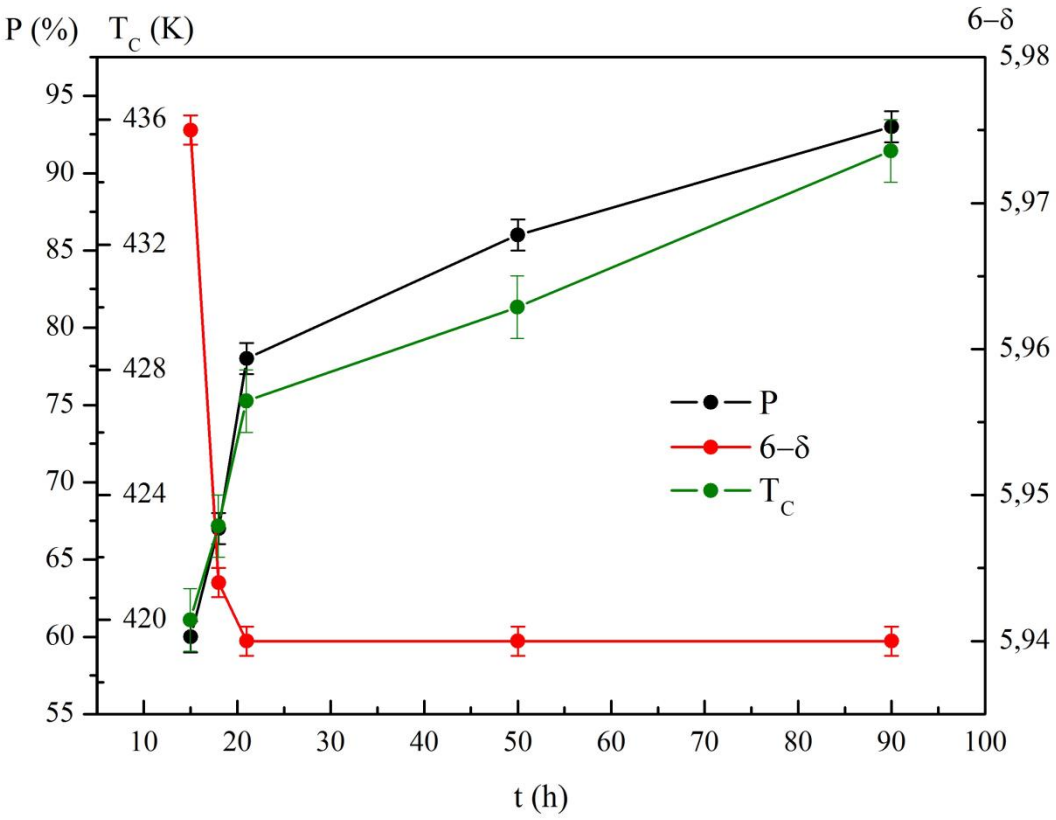

Figure 5

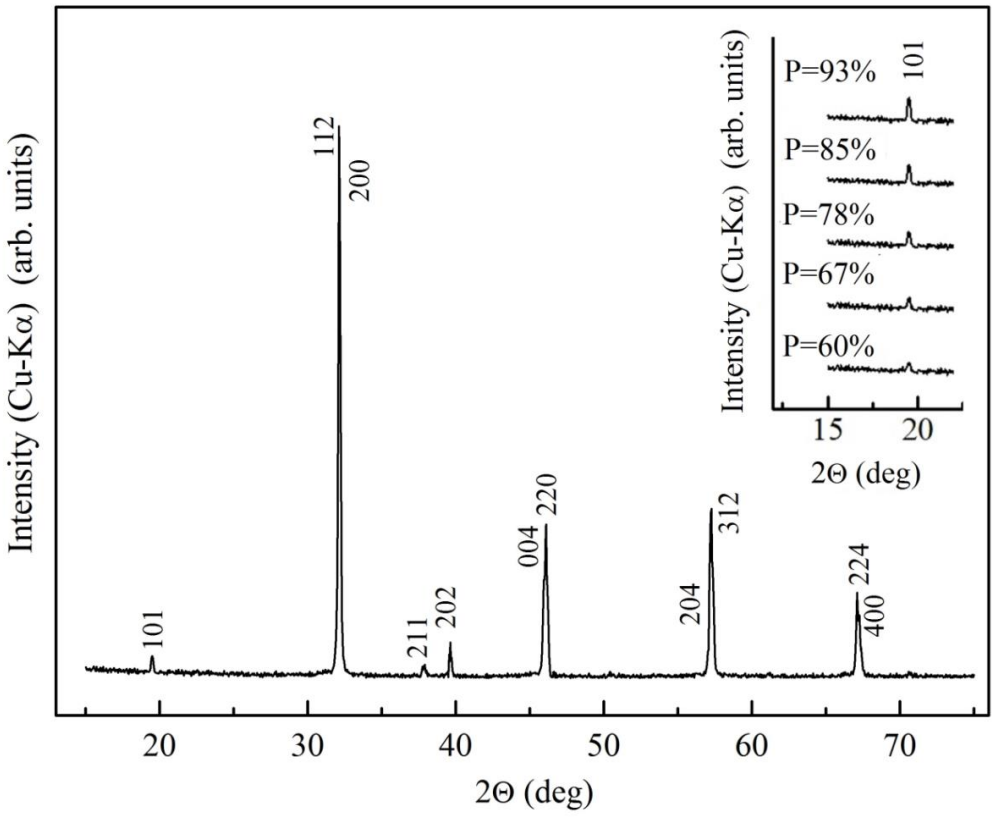

Figure 6

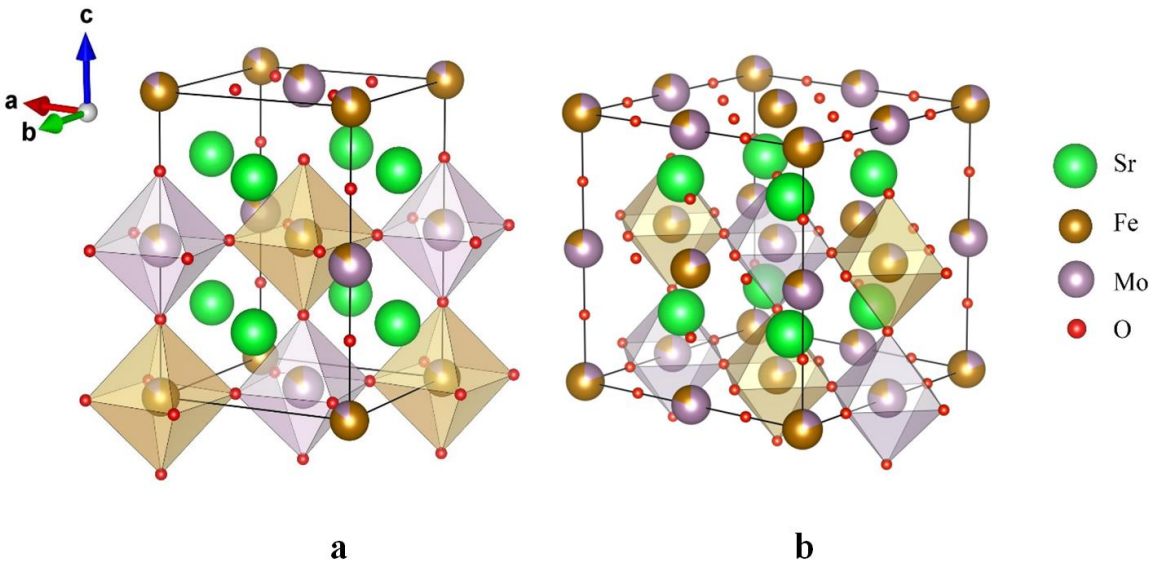
c
a
b
Sr
Fe
Mo
O
a
b

Figure 7

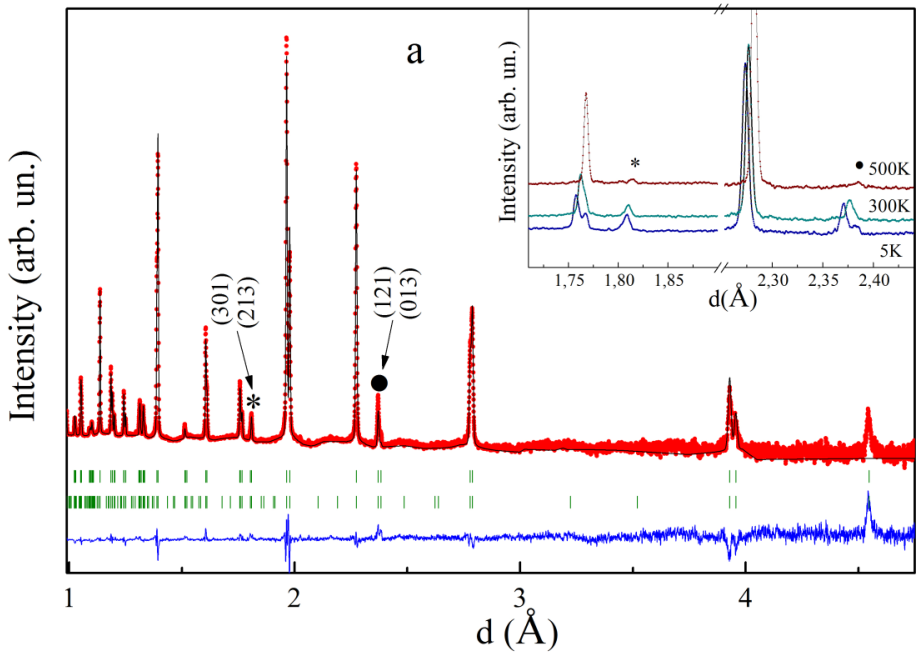
a
Intensity (arb. un.)
(301)
(213)
(121)
(013)
*
1
2
3
4
d (Å)
Intensity (arb. un.)
*
500K
300K
5K
1,75
1,80
1,85
2,30
2,35
2,40
d(Å)

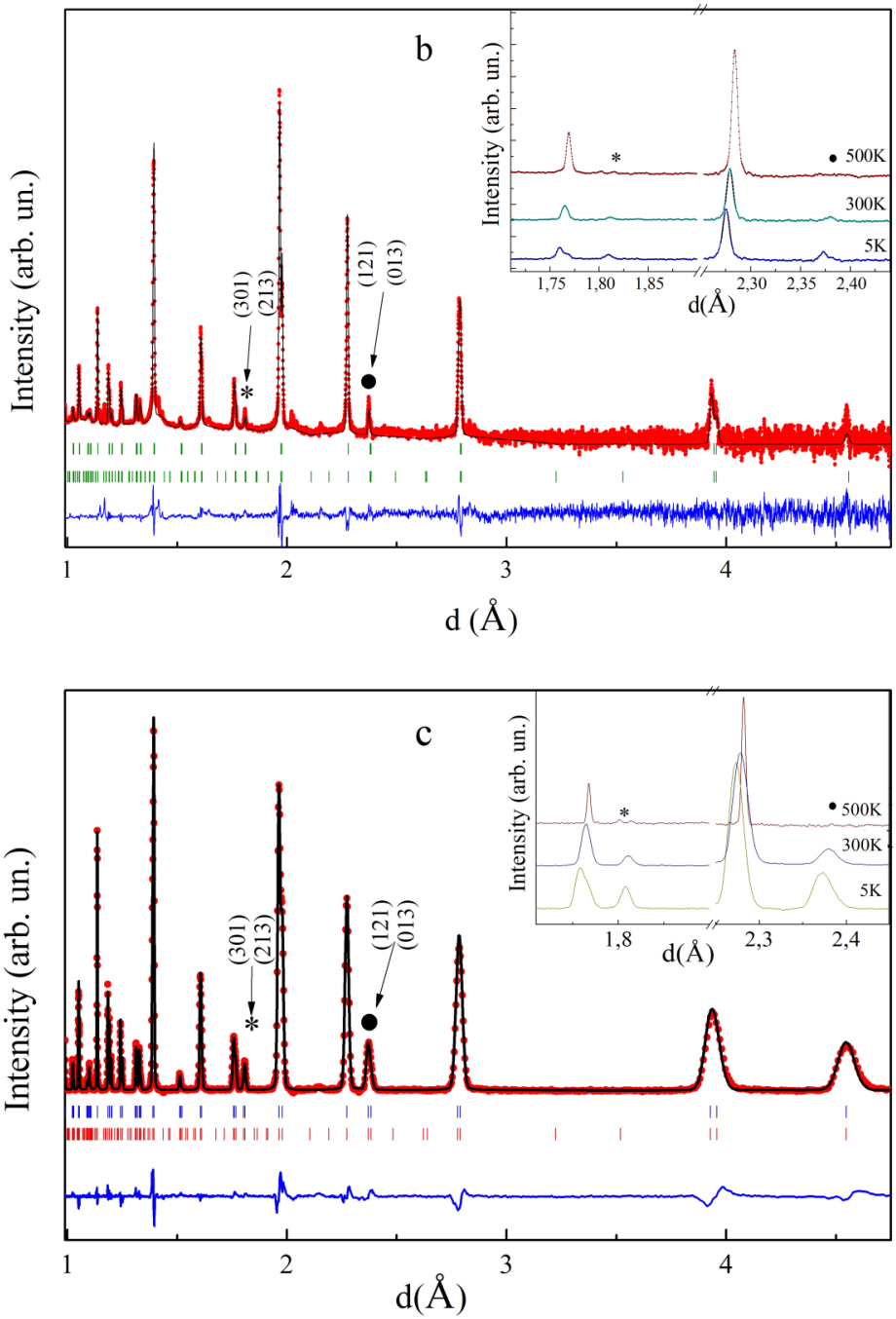
b
Intensity (arb. un.)
(301)
(213)
(121)
(013)
*
●
500K
300K
5K
1,75
1,80
1,85
2,30
2,35
2,40
d(Å)
1
2
3
4
d (Å)
c
Intensity (arb. un.)
(301)
(213)
(121)
(013)
*
●
500K
300K
5K
1,8
2,3
2,4
d(Å)
1
2
3
4
d(Å)

Figure 8

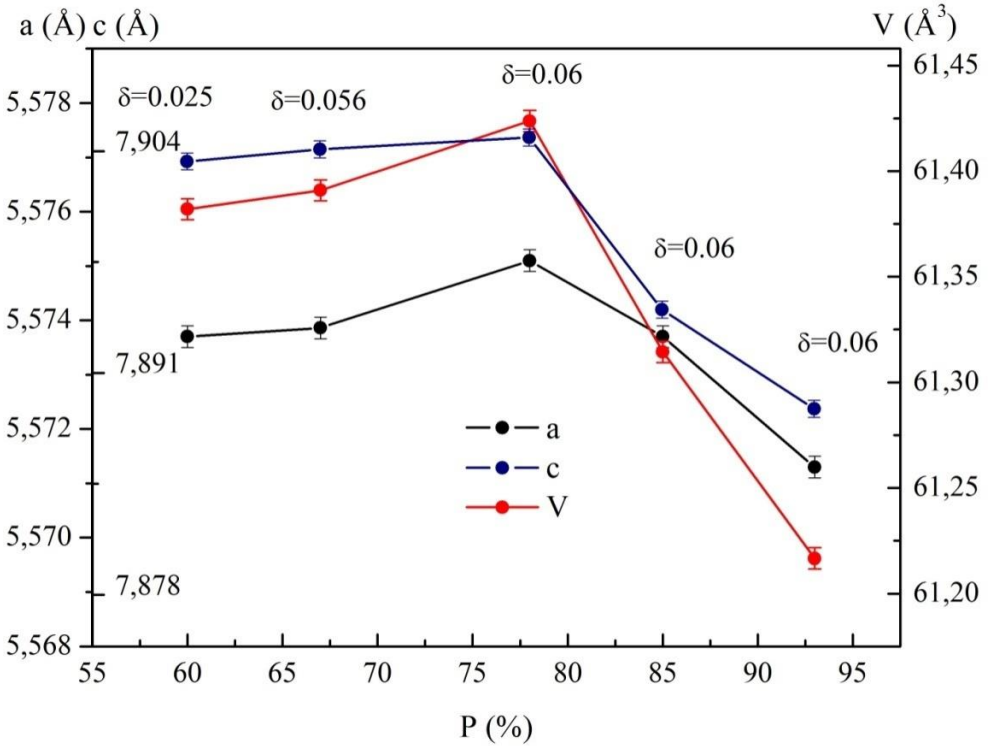

Figure 9

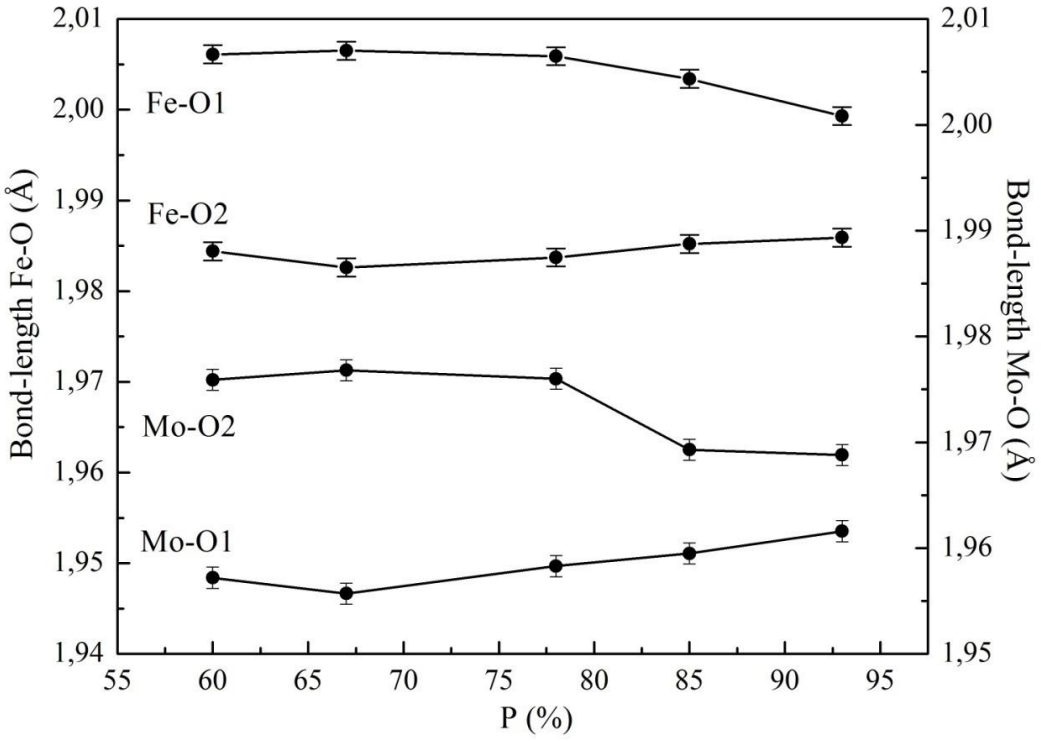

Figure 10

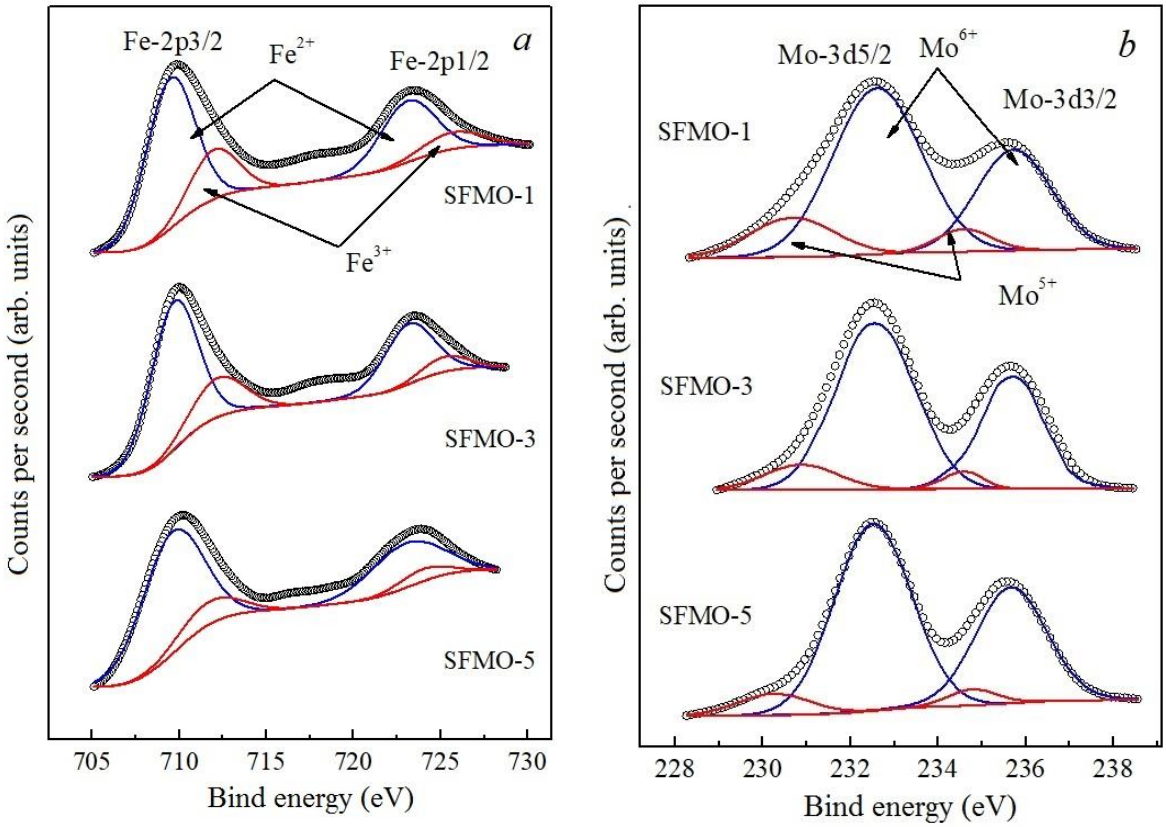

Figure 11

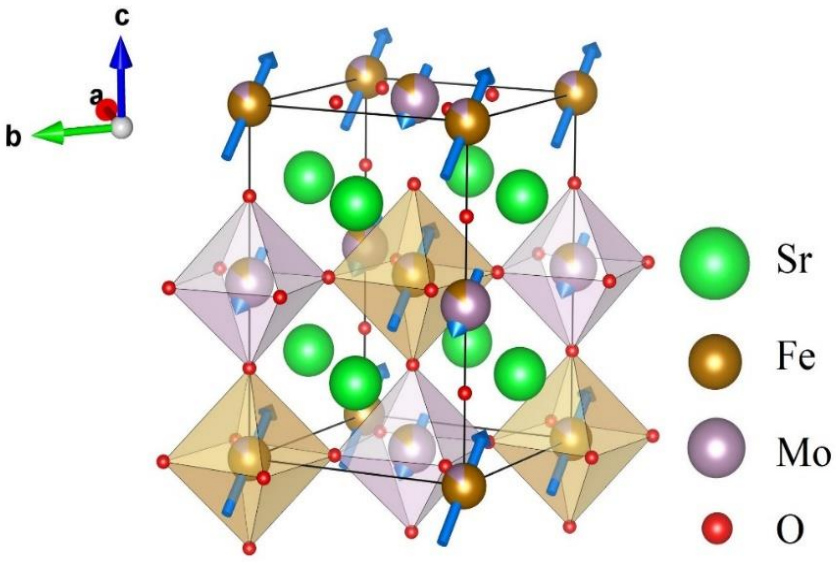

Figure 12

Table 1 Relaxation time of oxygen desorption process and the values of Fe/Mo cations ordering in the compounds $Sr_2FeMoO_{5.99(1)}$ annealed in the 5%H_2/Ar gaseous mixture with a heating rate of 12 K/min.

T, K	$6-\delta$	τ_o, s	dP_o/dt	τ_p, s
1320	5.97(8)	5.4320	0.4479	27.1173
1370	5.97(0)	5.0235	0.6458	25.8194
1420	5.94(1)	4.7411	0.7269	22.2838
1470	5.92(4)	2.7961	0.8191	19.7692

Table 2 The unit cell parameters (a, c), reduced unit cell volume (V_{red}=V/4 for tetragonal lattice, V_{red} = V/8 for cubic lattice), coordinates, bond lengths, angles and reliability factors calculated for the $Sr_2FeMoO_{6-\delta}$ compounds based on the neutron diffraction.

	SFMO–1 (P=60%)			SFMO–2 (P=67%)			SFMO–3 (P=78%)		
	I4/m T=5K	I4/m T=300 K	Fm –3m T=500 K	I4/m T=5K	I4/m T=300K	Fm –3m T=500K	I4/m T=5K	I4/m T=300K	Fm –3m T=500K
a (Å)	5.5566	5.5737	7.9059	5.5586	5.5739	7.9098	5.5550	5.5751	7.9051
c (Å)	7.9126	7.9034		7.91215	7.9041		7.91210	7.9048	
V_{red}(Å^3)	61.08	61.38	61.77	61.08	61.39	61.43	61.225	61.42	61.91
O1 (0,0,z)	0.2602	0.2581	0.2513	0.2697	0.2581	0.2504	0.23352	0.2356	0.2510
O2 (x)	0.2271	0.2327		0.2242	0.2327		0.2258	0.2290	
O2 (y)	0.2797	0.2752		0.2692	0.2752		0.2708	0.2643	
Fe–O1(Å)	1.9912	2.0061	2.1865	2.0813	2.0065	1.9782	2.0747	2.0059	1.9861
Fe–O2(Å)	1.9978	1.9844		1.9918	1.9826		1.9968	1.9837	
Mo–O1(Å)	1.9174	1.9572	1.9664	1.8919	1.9557	1.9717	1.9118	1.9583	1.9698
Mo–O2(Å)	1.9489	1.9759		1.9502	1.9768		1.9493	1.9760	
Fe/Mo (μ_B)	2.5/ –0.3	2.1/ –0.3	–	2.2/ –0.2	1.8/ –0.2		2.6/ –0.5	1.6/ –0.1	–
R_{wp}, %	3.19	5.10	5.25	5.84	5.21	5.07	4.47	4.34	4.62
χ^2	3.70	2.85	2.18	4.62	4.24	3.54	2.74	2.24	2.85

	SFMO –4 (P=85%)			SFMO –5 (P=93%)		
	I4/m T=5K	I4/m T=300K	Fm –3m T=500K	I4/m T=5K	I4/m T=300K	Fm –3m T=500K
a (Å)	5.54658	5.5737	7.90562	5.5382	5.5713	7.9038
c (Å)	7.8860	7.8947		7.8799	7.8889	
V_{red}(Å^3)	60.08	61.31	61.76	60.49	61.22	61.72
O1 (0,0,z)	0.2639	0.2539	0.2520	0.2619	0.2623	0.2525

O2 (x)	0.2337	0.2368		0.2238	0.2317	
O2 (y)	0.2623	0.2647		0.2719	0.2682	
Fe –O1(Å)	2.0071	2.0034	2.0094	1.9792	1.9993	2.0260
Fe –O2(Å)	1.9994	1.9852		2.0005	1.9859	
Mo – O1(Å)	1.9168	1.9595	1.9604	1.9238	1.9616	1.9559
Mo – O2(Å)	1.9469	1.9693		1.9440	1.9688	
Fe/Mo (μ_B)	3.2/ –0.5	2.2/ –0.3	–	3.9/ –0.5	2.5/ –0.4	–
R_{wp}, %	5.52	5.84	5.24	5.21	5.57	4.25
χ^2	4.12	3.54	3.62	3.24	3.95	2.84

Table 3 Binding energies of core levels of Fe_{2p} and Mo_{3d} ions, percentage of valence states of iron and molybdenum ions in the compounds $Sr_2FeMoO_{6-\delta}$ having different degree of the Fe/Mo cationic superstructural ordering.

Sample	$Mo3d_{5/2}$		$Mo3d_{3/2}$	
	Mo^{6+} (%)	Mo^{5+} (%)	Mo^{6+} (%)	Mo^{5+} (%)
SFMO –1	232.49 (69%)	230.20 (31%)	235.70 (69%)	234.86 (31%)
SFMO –3	232.54 (76%)	230.85 (24%)	235.67 (76%)	234.56 (24%)
SFMO –5	232.61 (84%)	230.58 (16%)	235.72 (84%)	234.58 (16%)
	$Fe3p_{3/2}$		$Fe3p_{1/2}$	
	Fe^{2+} (%)	Fe^{3+} (%)	Fe^{2+} (%)	Fe^{3+} (%)
SFMO –1	709.63 (72%)	712.10 (28%)	723.32 (72%)	725.96 (28%)
SFMO –3	709.91 (79%)	712.41 (21%)	723.24 (79%)	725.51 (21%)
SFMO –5	709.86 (83%)	712.21 (17%)	723.21 (83%)	724.34 (17%)